

# Threshold Effects in Multi-channel Coupling and Spectroscopic Factors in Exotic Nuclei

N. Michel<sup>†‡¶</sup>, W. Nazarewicz<sup>†‡§</sup>, M. Płoszajczak<sup>§</sup>

<sup>†</sup> *Department of Physics and Astronomy, University of Tennessee, Knoxville, TN 37996, USA*

<sup>‡</sup> *Physics Division, Oak Ridge National Laboratory, P.O. Box 2008, Oak Ridge, TN 37831, USA*

<sup>¶</sup> *Joint Institute for Heavy Ion Research, Oak Ridge, TN 37831, USA*

<sup>§</sup> *Institute of Theoretical Physics, Warsaw University, ul. Hoża 69, 00-681 Warsaw, Poland*

<sup>§</sup> *Grand Accélérateur National d'Ions Lourds (GANIL),  
CEA/DSM - CNRS/IN2P3, BP 55027, F-14076 Caen Cedex, France*

(Dated: May 20, 2018)

In the threshold region, the cross section and the associated overlap integral obey the Wigner threshold law that results in the Wigner-cusp phenomenon. Due to flux conservation, a cusp anomaly in one channel manifests itself in other open channels, even if their respective thresholds appear at a different energy. The shape of a threshold cusp depends on the orbital angular momentum of a scattered particle; hence, studies of Wigner anomalies in weakly bound nuclei with several low-lying thresholds can provide valuable spectroscopic information. In this work, we investigate the threshold behavior of spectroscopic factors in neutron-rich drip-line nuclei using the Gamow Shell Model, which takes into account many-body correlations and the continuum effects. The presence of threshold anomalies is demonstrated and the implications for spectroscopic factors are discussed.

PACS numbers: 21.10.Jx, 03.65.Nk, 21.60.Cs, 24.10.Cn, 24.10.Eq

In 1948, based on general principles, Wigner predicted [1] a characteristic behavior (a cusp) of scattering and reaction cross sections in the vicinity of a reaction threshold. This particular behavior (often referred to as the Wigner's threshold law or the Wigner-cusp phenomenon) was given a quantitative explanation a decade later [2, 3, 4, 5, 6, 7]. In particular, it has been noted [3, 4, 5, 6, 8] that, due to the unitarity of the scattering matrix and the resulting flux conservation, the presence of a threshold anomaly in an opening reaction channel can trigger an appearance of Wigner cusps in other open channels with lower thresholds. As the shape of the cusp strongly depends on orbital angular momentum (is strongest in  $s$  and  $p$  waves), it was early realized that the presence of cusp anomaly could provide structural information about reaction products [3, 4, 9].

The Wigner-cusp phenomenon has been studied experimentally and theoretically in various areas of physics: pion-nucleus scattering [9, 10], electron-molecule scattering [11], electron-atom scattering [12], and ultracold atom-diatom scattering [13]. In low-energy nuclear physics, threshold effects have been investigated in, e.g., charge-exchange reactions [14], neutron elastic scattering [15], and deuteron stripping [16]. Abramovich *et al.* [17] reviewed threshold phenomena in nuclear reactions, including those with the light neutron-rich systems such as  ${}^6\text{He}$ ,  ${}^{10}\text{Be}$ , and  ${}^{10}\text{Li}$  (see also Ref. [18]) that are of particular interest in the context of this work. The influence of threshold effects on the cross section and the strength function, hence the spectroscopic factor (SF) of a threshold state was pointed out in Refs. [8, 19].

The purpose of this study is many-fold. Firstly, we investigate whether the Wigner-cusp phenomenon appears naturally in a microscopic many-body approach rooted in an effective inter-nucleon interaction. The second goal

is to investigate the influence of threshold effects and the coupling to the non-resonant continuum on overlap integrals, or spectroscopic factors. We demonstrate that the energy dependence of SFs caused by an opening of a reaction channel can be described at the shell-model level only if nucleon-nucleon correlations involving scattering states are treated properly. Finally, we emphasize the importance of experimental studies of cusp phenomena in weakly bound, neutron-rich nuclei in which low-lying one-neutron and two-neutron thresholds appear.

The traditional shell model (SM) of nuclear structure views the nucleus as a closed quantum system (CQS) in which nucleons occupy bound orbits. While such an assumption may be somehow justified for well-bound nuclei having high particle-emission thresholds, it can no longer be applied to weakly bound or unbound systems in the vicinity of drip lines, where the coupling to the particle continuum (both resonances and the non-resonant scattering states) becomes important. This coupling can be considered in the open quantum system (OQS) extension of the SM, the so-called continuum SM (see Ref. [20] for a recent review). In this work, we apply the complex-energy implementation of the continuum SM, the so-called Gamow Shell Model (GSM) [21, 22] in the version of Refs. [21, 23]. GSM is a multi-configurational SM with a single-particle (s.p.) basis given by the Berggren ensemble [24] which consists of Gamow (bound and resonance) states and the non-resonant continuum. For a given Hamiltonian, the number of particles occupying states of the non-resonant continuum is a result of GSM variational calculations. The resonant states of the GSM are the generalized eigenstates of the time-independent Schrödinger equation which are regular at the origin and satisfy purely outgoing boundary conditions. The GSM can thus be viewed as a quasi-stationary many-body OQS

formalism. (An alternative microscopic approach, successfully applied to the structure of weakly bound or unbound nuclei, is the Complex Scaling Method that is capable of treating different kinds of reaction channels and continuum states starting from different thresholds [25].) Since the Wigner-cusp phenomenon is most pronounced for low- $\ell$  waves and for neutrons (no Coulomb barrier), as an illustrative example we choose the case of the one-neutron (1n) channel in the model two- and three-neutron systems outside the inert core:  ${}^6\text{He}$  and  ${}^7\text{He}$ . Our aim is not to fit the actual experimental data, but rather to accomplish the physics goals as stated above.

*Gamow Shell Model Framework*– The starting point of GSM is the Berggren one-body completeness relation [24] allowing the expansion of both bound and unbound states. The Berggren ensemble consists of resonant and scattering states generated by a finite-depth potential  $V(r)$ . Resonant states are solutions of the Schrödinger equation with purely outgoing asymptotics. Their energies and wave functions are in general complex. The resonant states of the GSM have either bound or decaying character; they form the so-called *pole subspace*. Scattering states entering the Berggren ensemble are also defined in the complex energy/momentum plane. For a given partial wave  $(\ell, j)$ , the scattering states are distributed along a contour  $L_+^{\ell j}$  in the complex momentum plane. The set of all bound and decaying states  $|u_n\rangle$  enclosed between  $L_+^{\ell j}$  and the real  $k$ -axis, and scattering states  $|u_k\rangle$  in  $L_+^{\ell j}$  is complete [24]:

$$\sum_{\mathcal{B}}^{\dagger} |u_{\mathcal{B}}\rangle \langle \widetilde{u}_{\mathcal{B}}| = 1, \quad (1)$$

where  $|\mathcal{B}\rangle$  is either a discrete resonant state or a scattering continuum state ( $L_+^{\ell j}$  part). The tilde symbol above bra vectors in Eq. (1) signifies that the complex conjugation arising in the dual space affects only the angular part and leaves the radial part unchanged [24]. The continuous part of the completeness relation (1) has to be discretized in numerical applications. For that purpose, scattering states are discretized and renormalized in order to obtain a discrete completeness relation [24]:

$$\sum_{\mathcal{B}=1}^N |u_{\mathcal{B}}\rangle \langle \widetilde{u}_{\mathcal{B}}| \simeq 1 \quad ; \quad |u_{\mathcal{B}}\rangle = \sqrt{\omega_{\mathcal{B}}} |u_{k_{\mathcal{B}}}\rangle, \quad (2)$$

where  $\{k_{\mathcal{B}}, \omega_{\mathcal{B}}\}$  is the set of discretized momenta and associated weights provided by a Gauss-Legendre quadrature. The many-body GSM basis corresponds to Slater determinants (SD) spanned by one-body Berggren states:  $|SD_i\rangle = |u_{i_1} \cdots u_{i_A}\rangle$  where  $|SD_i\rangle$  is the  $i$ -th SD in the  $A$ -body basis and  $u_{i_j}$  is the  $j$ -th one-body state occupied in  $|SD_i\rangle$ . The many-body completeness relation is built from Eq. (2) by forming all possible SDs generated by the Gamow one-body states:

$$\sum_i |SD_i\rangle \langle \widetilde{SD}_i| \simeq 1. \quad (3)$$

The completeness in (3) is not exact as the one-body completeness relation (2) is approximate due to the discretization. In the basis (3), the GSM Hamiltonian  $H$  becomes a complex symmetric matrix. Moreover, many-body bound and resonant states are embedded in the background of non-resonant scattering eigenstates, so that one needs a criterion to isolate them. The overlap method [21] has proven to be very efficient to solve this problem. For this, one diagonalizes first  $H$  in the pole subspace to generate a zeroth-order vector  $|\Psi_0\rangle$ . In the second step,  $|\Psi_0\rangle$  is used as a pivot to generate a Lanczos subspace of the full GSM space. Its diagonalization provides eigenvectors of  $H$  in the total GSM space, and the requested bound or decaying eigenstate of  $H$  is the one which maximizes the overlap  $|\langle \Psi_0 | \Psi \rangle|$ .

The definition of observables in GSM follows directly from the mathematical setting of quantum mechanics in the rigged Hilbert space rather than the usual Hilbert space [26, 27]. Modified definition of the dual space, embodied by the tilde symbol above bra states, implies that observables in many-body resonances become complex. In this case, the real part of a matrix element corresponds to the expectation value, and the imaginary part can be interpreted as the uncertainty in the determination of this expectation value due to the possibility of decay of the state during the measuring process [24, 28].

*GSM Hamiltonian*– In this Letter, the s.p. basis (1) is generated by a Woods-Saxon (WS) potential with the radius  $R_0=2$  fm, the diffuseness  $d=0.65$  fm, the spin-orbit strength  $V_{so}=7.5$  MeV, and the depth of the central potential  $V_0=47$  MeV (the “ ${}^5\text{He}$ ” parameter set). This potential reproduces experimental energies and widths of the s.p. resonances  $3/2_1^-$  and  $1/2_1^-$  in  ${}^5\text{He}$ . The GSM Hamiltonian is a sum of the one-body WS potential, representing the effect of an inert  ${}^4\text{He}$  core, and of the two-body interaction among valence particles, given by a finite-range surface Gaussian interaction (SGI) [23] with the range  $\mu = 1$  fm and the coupling constants depending on the total angular momentum  $J$  of the neutron pair:  $V_0^{(0)} = -403$  MeV fm<sup>3</sup> and  $V_0^{(2)} = -392$  MeV fm<sup>3</sup>. These constants are fitted to reproduce the experimental ground state (g.s.) binding energies of  ${}^6\text{He}$  and  ${}^7\text{He}$  with the “ ${}^5\text{He}$ ” WS potential. The valence space for neutrons consists of the  $p_{3/2}$  and  $p_{1/2}$  partial waves. The  $p_{3/2}$  wave functions include a  $0p_{3/2}$  resonant state and  $p_{3/2}$  non-resonant scattering states along a complex contour enclosing the  $0p_{3/2}$  resonance in the complex  $k$ -plane. For a  $p_{1/2}$  part, we take non-resonant scattering states along the real- $k$  axis (the broad  $0p_{1/2}$  resonant state plays a negligible role in the g.s. wave function of  ${}^6\text{He}$ ). For both contours, the maximal momentum value is  $k_{\max} = 3.27$  fm<sup>-1</sup>. The contours have been discretized with up to 60 points and the attained precision on energies and widths is better than 0.1 keV. In the subsequent analysis, parameters of the GSM Hamiltonian are varied in order to change positions of 1n thresholds in various isotopes.

In order to illuminate the continuum coupling effects in

GSM, we have introduced a simplified harmonic oscillator SM (HO-SM) scheme. Here, the radial wave functions are those of the spherical harmonic oscillator with the frequency  $\hbar\omega = 41A^{-1/3}$  MeV. The one-body part of the HO-SM Hamiltonian is given by the real energies of the one-body part of the GSM Hamiltonian. The HO-SM scheme is supposed to illustrate the “standard” CQS SM calculations in which only bound valence shells are considered in the s.p. basis.

*Spectroscopic Factors in GSM*– SFs are useful indicators of the configuration mixing in the many-body wave function. Extensive attempts have been made to deduce SFs using direct reactions, such as single-nucleon transfer, nucleon knockout, and elastic break-up reactions, using hadronic and leptonic probes. These analyses often reveal model- and probe-dependence [29, 30, 31] raising concerns about the possibility of their precise experimental determination. (For an extensive study of spectroscopic factors in exotic nuclei from nucleon-knockout reactions, see Ref. [32].) Studies of  $(e, e'p)$  reactions in closed-shell nuclei [33] demonstrated that the SFs are reduced by  $\sim 35\%$  with respect to the standard SM predictions, mainly due to the coupling to high-momentum states reached by the short-range and tensor components of the nucleon-nucleon interaction [34]. In this work, we point out that additional difficulties in extracting and interpreting SFs from the measured cross sections using the standard SM lie in the neglect of particle continuum, channel coupling, and strength fragmentation.

Single-nucleon overlap integrals and the associated spectroscopic factors (SFs) are basic ingredients of the theory of direct reactions (single-nucleon transfer, nucleon knockout, elastic break-up) [35, 36]. Experimentally, SFs can be deduced from measured cross sections; they are useful measures of the configuration mixing in the many-body wave function. The associated reaction-theoretical analysis often reveals model- and probe-dependence [29, 30, 31] raising concerns about the accuracy of experimental determination of SFs. In our study we discuss the uncertainty in determining SFs due to the two assumptions commonly used in the standard SM studies, namely (i) that a nucleon is transferred to/from a specific s.p. orbit (corresponding to an observed s.p. state), and (ii) that the transfer to/from the continuum of non-resonant scattering states can be disregarded. In this work, we define SFs in a usual way, through the radial overlap functions  $u_{\ell j}(r)$  [36, 37, 38]:

$$u_{\ell j}(r) = \langle \Psi_A^{JA} | [ |\Psi_{A-1}^{JA-1} \rangle \otimes | \ell, j \rangle ]^{JA} \rangle, \quad (4)$$

where  $|\Psi_A^{JA} \rangle$  and  $|\Psi_{A-1}^{JA-1} \rangle$  are wave functions of nuclei  $A$  and  $A-1$ , respectively, and  $| \ell, j \rangle$  is the angular-spin part of the channel function. The angular-spin degrees of freedom are integrated out in Eq. (4) so that  $u_{\ell j}$  depends only on the relative radial coordinate of the transferred particle  $r = |\vec{r}|$ . The spectroscopic factor, denoted by  $S^2$ , is defined as usual through the norm of the overlap function [36, 37, 38]. Using a decomposition of the  $(\ell, j)$

channel function in the complete Berggren basis, one obtains:

$$u_{\ell j}(r) = \sum_{\mathcal{B}} \langle \widetilde{\Psi}_A^{JA} | a_{\ell j}^+(\mathcal{B}) | \Psi_{A-1}^{JA-1} \rangle \langle r \ell j | \mathcal{B} \rangle, \quad (5)$$

$$S^2 = \sum_{\mathcal{B}} \langle \widetilde{\Psi}_A^{JA} | a_{\ell j}^+(\mathcal{B}) | \Psi_{A-1}^{JA-1} \rangle^2, \quad (6)$$

where  $a_{\ell j}^+(\mathcal{B})$  is a creation operator associated with a s.p. Berggren state  $|\mathcal{B}\rangle$ . Since Eqs. (5,6) involve summation over all discrete Gamow states and integration over all scattering states along the contour  $L_{\pm}^{\ell j}$ , the final result is independent of the s.p. basis assumed. This is in contrast to standard SF experimental extraction and SM calculations where model-dependence enters through the specific choice of a s.p. state  $a_{n\ell j}^+$ , with Eq. (6) reducing to the sole matrix element  $\langle \Psi_A^{JA} | a_{n\ell j}^+ | \Psi_{A-1}^{JA-1} \rangle^2$ . This can lead to sizeable errors if the states of  $A-1$  and/or  $A$  lie close to a channel threshold.

*The Threshold Cusp*– The GSM results for  ${}^6\text{He}$  g.s. SF in the channel:  $[{}^5\text{He}(\text{g.s.}) \otimes p_{3/2}]^{0+}$  are shown in Fig. 1a as a function of one-neutron separation energy  $S_{1n}$  in  ${}^6\text{He}$ . To this end, we have fixed the depth of the WS potential so that  $0p_{3/2}$  and  $0p_{1/2}$  are both bound with respective energies  $-5$  and  $-0.255$  MeV, and we have varied the SGI monopole coupling constant  $V_0^{(J=0)}$  so that the 1n separation energy of  ${}^6\text{He}$  goes through zero. At  $S_{1n}=0$  (1n-emission threshold), the calculated SF exhibits behavior consistent with the Wigner threshold law: the quickly varying component of SF behaves as  $(-S_{1n})^{\ell-1/2}$  ( $\ell=1$ ) below the 1n threshold and follows the  $(S_{1n})^{\ell+1/2}$  rule above the threshold. It is worth noting that the parameters of the GSM Hamiltonian and the associated S-matrix poles do not show any discontinuities around  $S_{1n}=0$ . This result constitutes an excellent test of the GSM formalism: the Wigner limit is reached precisely at the 1n threshold obtained from many-body calculations. It is interesting to see that the HO-SM results are depressed by about 25% as compared to GSM. Indeed, in the HO-SM s.p. basis, the configurations  $[0p_{3/2} \otimes 0p_{3/2}]^{0+}$  and  $[0p_{1/2} \otimes 0p_{1/2}]^{0+}$  are strongly mixed by the SGI residual interaction; hence, the value of  $p_{3/2}$  SF in the g.s. of  ${}^6\text{He}$  is significantly reduced. Moreover, the s.p. basis in HO-SM calculations comprises HO states whose radial form factors are independent of the depth of the WS potential. Hence, no threshold effect can be seen in HO-SM SFs.

*Threshold Effects Due to Channel Coupling*– As discussed above, when a new channel opens at energy  $E_t$ , there appears a flux redistribution in other open channels with lower thresholds. This flux redistribution may be affected by the presence of the Wigner cusp in the new channel; hence, the reaction cross-sections in all open channels may exhibit the threshold anomaly at  $E_t$ . To illustrate the phenomenon of channel coupling, Fig. 1b shows again the SF for the  $[{}^5\text{He}(\text{g.s.}) \otimes p_{3/2}]^{0+}$  channel

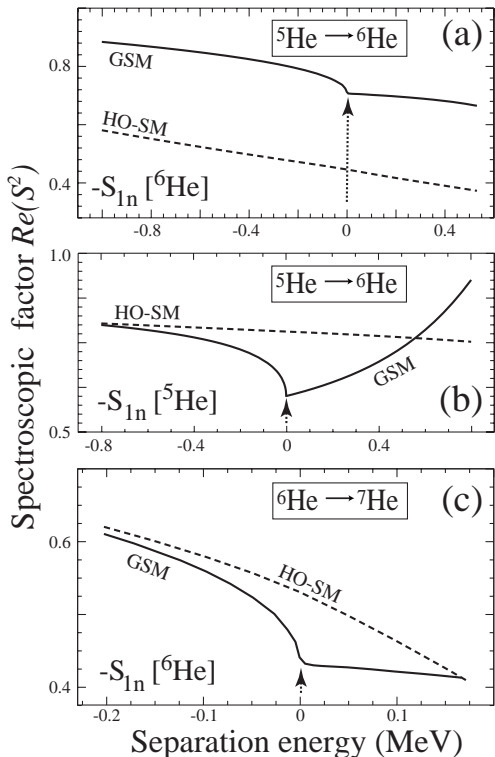


FIG. 1: The real part of the overlap integral as a function of one-neutron separation energy  $S_{1n}$  as indicated. Top and middle:  $({}^6\text{He}(\text{g.s.})|{}^5\text{He}(\text{g.s.}) \otimes p_{3/2})^{0+}$ ; bottom:  $({}^7\text{He}(\text{g.s.})|{}^6\text{He}(\text{g.s.}) \otimes p_{3/2})^{0+}$ . Solid line: GSM results; dashed line: the SM approximation (HO-SM) where the SGI matrix elements are calculated in the HO basis  $\{0p_{3/2}, 0p_{1/2}\}$ . The 1n thresholds in  ${}^6\text{He}$  (top and bottom) and  ${}^5\text{He}$  are marked by arrows. The results displayed in the middle panel are plotted as a function of the energy of the  $0p_{3/2}$  resonant state, which, in our model, is negative of  $S_{1n}[{}^5\text{He}]$ . For more details, see the discussion in the text.

but this time as a function of the  $0p_{3/2}$  s.p. state energy (or negative  $S_{1n}$  of  ${}^5\text{He}$ ). This calculation was carried out by varying the depth of the WS potential so that the  $p_{3/2}$  pole of the  $S$ -matrix (which is also the g.s. of  ${}^5\text{He}$  in our model space), would change its character from a bound state to an unbound decaying Gamow state. At  $S_{1n}[{}^5\text{He}]=0$ , the 1n and 2n thresholds in  ${}^6\text{He}$  become degenerate, i.e., the two channels of  ${}^5\text{He}+n$ , namely  ${}^6\text{He}$  and  ${}^4\text{He}+2n$  couple. As seen in Fig. 1, the SF in the  $[{}^5\text{He}(\text{g.s.}) \otimes p_{3/2}]^{0+}$  channel exhibits the Wigner cusp at  $S_{1n}[{}^5\text{He}]=0$ , i.e., at a 2n threshold. At this point, the first derivative  $\partial S^2/\partial e_{0p_{3/2}}$  of the SF becomes infinite, consistent with the Wigner law for  $\ell=1$ . The SF in HO-SM varies very little in the whole studied range of  $0p_{3/2}$  energies. (Let us mention that the competition between bound and unbound states in  ${}^6\text{He}$ , and the  ${}^5\text{He}+n$  and  ${}^4\text{He}+2n$  reaction channels has been studied within the

coupled cluster method [25].)

In the case shown in Fig. 1b the GSM Hamiltonian changes at  $S_{1n}[{}^5\text{He}]=0$  as at this point the  $0p_{3/2}$  pole becomes unbound. It is, therefore, instructive to investigate the situation at which the Hamiltonian behaves smoothly around the threshold. Figure 1c illustrates the case of  ${}^7\text{He}$  g.s. in the channel  $[{}^6\text{He}(\text{g.s.}) \otimes p_{3/2}]^{3/2-}$ . In order to avoid secondary open-channel mixing effects, we have adjusted the WS potential depth so that the  ${}^5\text{He}$  g.s. is bound by 5 MeV and cannot play any role in the anomalous energy dependence of the studied SF. The  $0p_{1/2}$  state is weakly bound with an energy of  $-0.255$  MeV. In order to control the binding energy of  ${}^6\text{He}$ , the  $V_0^{(J=0)}$  coupling constant is varied so that  ${}^7\text{He}$  g.s. is always bound while  $S_{1n}$  of  ${}^6\text{He}$  goes through zero. The GSM space is the same as in the previous cases, except that the  $0p_{1/2}$  state is now included in the GSM basis as it is bound. A cusp in the calculated SF for  ${}^7\text{He}$  is clearly seen at  $S_{1n}[{}^6\text{He}]=0$ . The threshold anomaly shown in Fig. 1c can only result from the cross-channel couplings. Again, the SF in HO-SM smoothly varies in the whole energy region considered.

*Conclusions*– The anomalies in the spectroscopic factors when the total energy of the system varies through the threshold of an opening channel are discussed within the many-body OQS formalism of the GSM. The main conclusions of this work can be summarized as follows: (i) Many-body OQS calculations correctly predict the Wigner-cusp and channel-coupling threshold effects. This constitutes a very strong theoretical check for the GSM approach; (ii) The spectroscopic factors defined in the OQS framework through the norm of the overlap integral, exhibit strong variations around particle thresholds. Such variations cannot be described in a standard CQS SM framework that applies a ‘one-isolated-state’ ansatz and ignores the coupling to the decay and scattering channels. In our model calculations, the contribution to SF from a non-resonant continuum can be as large as 25%; (iii) Any theoretical model aiming at a meaningful description of SFs of low- $\ell$  states in weakly bound nuclei must meet certain minimal conditions. Namely, it should be able to account for (a) many-body configuration mixing and the resulting spreading of the spectroscopic strength due to inter-nucleon correlations, (b) coupling to the particle continuum that affects radial properties of wave functions in the neighborhood of reaction thresholds, and (c) coupling between various reaction channels.

Considering points (ii) and (iii) above, one should be careful when extracting spectroscopic information from transfer experiments on drip-line nuclei. The results presented in this work suggest that, similar to other fields, experimental studies of various aspects of threshold effects could provide valuable spectroscopic information about the s.p. structure of weakly bound nuclei. Here, of particular interest are systems with near-lying 1n and 2n thresholds such as  ${}^6,8\text{He}$  or non-Borromean two-neutron halos [39], in which cusps in SFs are expected to be par-

ticularly strong in low- $\ell$  ( $\ell = 0, 1$ ) neutron channels. Similar features were found in the analysis of the continuum-coupling correction to the CQS eigenvalues near the reaction threshold [40]. Finally, let us note that a threshold anomaly is also expected in proton-rich nuclei. While the effect is weaker than in the neutron-rich systems, one still expects anomalous differences in SFs and other spectroscopic quantities in mirror nuclei. Work along these lines

is in progress.

This work was supported by the U.S. Department of Energy under Contract Nos. DE-FG02-96ER40963 (University of Tennessee), DE-AC05-00OR22725 with UT-Battelle, LLC (Oak Ridge National Laboratory), and DE-FG05-87ER40361 (Joint Institute for Heavy Ion Research).

- 
- [1] E.P. Wigner, Phys. Rev. **73**, 1002 (1948).  
 [2] G. Breit, Phys. Rev. **107**, 1612 (1957).  
 [3] A.I. Baz, Soviet Phys. - JETP **6**, 709 (1957).  
 [4] R.G. Newton, Phys. Rev. **114**, 1611 (1959).  
 [5] W.E. Meyerhof, Phys. Rev. **129**, 692 (1963).  
 [6] A.I. Baz, Y.B. Zeldovich, and A.M. Peremolov, *Scattering, Reactions and Decays in Nonrelativistic Quantum Mechanics*, (Jerusalem, 1969, translated from Russian, Nauka, Moscow, 1966).  
 [7] A.M. Lane, Phys. Lett. B **33**, 274 (1970).  
 [8] C. Hategan, Annals of Physics **116** 77 (1978).  
 [9] R.K. Adair, Phys. Rev. **111**, 632 (1958).  
 [10] A. Starostin *et al.*, Phys. Rev. C **72**, 015205 (2005).  
 [11] W. Domcke, J. Phys. B **14**, 4889 (1981).  
 [12] K.F. Scheibner, A. U. Hazi, and R.J.W. Henry, Phys. Rev. A **35**, 4869 (1987).  
 [13] R.C. Forrey, N. Balakrishnan, V. Kharchenko, and A. Dalgarno, Phys. Rev. A **58**, R2645 (1998).  
 [14] P.R. Malmberg, Phys. Rev. **101**, 114 (1956).  
 [15] J.T. Wells, A.B. Tucker, and W.E. Meyerhof, Phys. Rev. **131**, 1644 (1963).  
 [16] C.F. Moore *et al.*, Phys. Rev. Lett. **17**, 926 (1966).  
 [17] S. Abramovich, B. Guzhovskij, and L. Lasarev, Sov. J. Part. Nucl. **23**, 129 (1992).  
 [18] C. Hategan, Proc. Rom. Acad. A **3** 11 (2002).  
 [19] G. Graw and C. Hategan, Phys. Lett. B **37** 41 (1971).  
 [20] J. Okołowicz, M. Płoszajczak, and I. Rotter, Phys. Rep. **374**, 271 (2003).  
 [21] N. Michel, W. Nazarewicz, M. Płoszajczak, and K. Benaceur, Phys. Rev. Lett. **89**, 042502 (2002); N. Michel, W. Nazarewicz, M. Płoszajczak, and J. Okołowicz, Phys. Rev. C **67**, 054311 (2003).  
 [22] R. Id Betan, R.J. Liotta, N. Sandulescu, and T. Vertse, Phys. Rev. Lett. **89**, 042501 (2002); Phys. Rev. C **67**, 014322 (2003).  
 [23] N. Michel, W. Nazarewicz, and M. Płoszajczak, Phys. Rev. C **70**, 064313 (2004).  
 [24] T. Berggren, Nucl. Phys. A **109**, 265 (1968).  
 [25] T. Myo, K. Katō, S. Aoyama, and K. Ikeda, Phys. Rev. C **63**, 054313 (2001).  
 [26] A. Bohm, *The Rigged Hilbert Space and Quantum Mechanics*, Lecture Notes in Physics **78** (Springer, New York 1978).  
 [27] R. de la Madrid, Eur. J. Phys. **26**, 287 (2005).  
 [28] O. Civitarese, M. Gadella, and R. Id Betan, Nucl. Phys. A **660**, 255 (1999).  
 [29] P.M. Endt, Atomic Data and Nuclear Data Tables **19**, 23 (1977); M.B. Tsang, Jenny Lee, and W.G. Lynch, Phys. Rev. Lett. **95**, 222501 (2005).  
 [30] G.J. Kramer, H.P. Blok, and L. Lapikas, Nucl. Phys. A **679**, 267 (2001).  
 [31] B.A. Brown, P.G. Hansen, B.M. Sherrill, and J.A. Tostevin, Phys. Rev. C **65**, 061601(R) (2002); P.G. Hansen and J.A. Tostevin, Ann. Rev. Nucl. Part. Sci. **53**, 219 (2003).  
 [32] A. Gade *et al.*, Phys. Rev. Lett. **93**, 042501 (2004); Eur. Phys. J. A **25**, s1.251 (2005).  
 [33] A.E.L. Dieperink and P. de Witt Huberts, Ann. Rev. Nucl. Part. Sci. **40**, 239 (1990); I. Sick and P. de Witt Huberts, Commun. Nucl. Part. Phys. **20**, 177 (1991); L. Lapikas, Nucl. Phys. A **553**, 297c (1993).  
 [34] W.H. Dickhoff and C. Barbieri, Prog. Part. Nucl. Phys. **52**, 377 (2004).  
 [35] G.R. Satchler, *Direct Nuclear Reactions* (Clarendon, Oxford, 1983).  
 [36] M.H. Macfarlane and J.B. French, Rev. Mod. Phys. **32**, 567 (1960).  
 [37] N.K. Glendenning, *Direct Nuclear Reactions* (Academic Press inc., 1983).  
 [38] P. Fröbrich and R. Lipperheide, *Theory of Nuclear Reactions* (Oxford Science Publications, Clarendon Press Oxford, 1996).  
 [39] N.K. Timofeyuk, L.D. Blokhintsev, and J.A. Tostevin, Phys. Rev. C **68** 021601(R) (2003).  
 [40] N. Michel, W. Nazarewicz, J. Okołowicz, and M. Płoszajczak, Nucl. Phys. A **752**, 335c (2005); Y. Luo, J. Okołowicz, M. Płoszajczak, and N. Michel, arXiv:nucl-th/0201073.